IEEE Access
Multidisciplinary ⋮ Rapid Review ⋮ Open Access Journal

Received October 30, 2018, accepted November 18, 2018, date of publication January 2, 2019, date of current version January 16, 2019.

Digital Object Identifier 10.1109/ACCESS.2018.2883957

Neural Network Based Brain Tumor Detection Using Wireless Infrared Imaging Sensor

P. MOHAMED SHAKEEL[1], TAREK E. EL. TOBELY[2], HAYTHAM AL-FEEL[3], GUNASEKARAN MANOGARAN[4], AND S. BASKAR[5]

[1]Faculty of Information and Communication Technology, Universiti Teknikal Malaysia Melaka, Durian Tunggal 76100, Malaysia
[2]Computer Engineering and Automatic Control Department, Faculty of Engineering, Tanta University, Tanta, Egypt
[3]Faculty of Computers & Information, Fayoum University, Fayoum, Egypt
[4]University of California at Davis, Davis, CA 95616, USA
[5]Department of ECE, Karpagam Academy of Higher Education, Coimbatore 641021, India

Corresponding author: P. Mohamed Shakeel (shakeelji@ieee.org)

ABSTRACT Now-a-days image processing placed an important role for recognizing various diseases such as breast, lung, and brain tumors in earlier stage for giving the appropriate treatment. Presently, most cancer diagnosis worked according to the visual examination process with effectively. Human visual reviewing of infinitesimal biopsy pictures is exceptionally tedious, subjective, and conflicting due to between and intra-onlooker varieties. In this manner, the malignancy and it's compose will be distinguished in a beginning time for finish treatment and fix. This brain tumor classification system using machine learning-based back propagation neural networks (MLBPNN) causes pathologists to enhance the exactness and proficiency in location of threat and to limit the entomb onlooker variety. Moreover, the technique may assist doctors with analyzing the picture cell by utilizing order and bunching calculations by recoloring qualities of the phones. The different picture preparing steps required for disease location from biopsy pictures incorporate procurement, upgrade, and division; include extraction, picture portrayal, characterization, and basic leadership. In this paper, MLBPNN is analyzed with the help of infra-red sensor imaging technology. Then, the computational multifaceted nature of neural distinguishing proof incredibly diminished when the entire framework is deteriorated into a few subsystems. The features are extracted using fractal dimension algorithm and then the most significant features are selected using multi fractal detection technique to reduce the complexity. This imaging sensor is integrated via wireless infrared imaging sensor which is produced to transmit the tumor warm data to a specialist clinician to screen the wellbeing condition and for helpful control of ultrasound measurements level, especially if there should arise an occurrence of elderly patients living in remote zones.

INDEX TERMS Wireless infrared imaging sensor, infra-red sensor, principal component analysis gray level covariance matrix, machine learning based neural networks.

I. INTRODUCTION

In the developing technology normal-abnormal classification of MRI brain images proposes, a level based approach, and compares the result with the existing methods. The existing works does not consider the anatomical structure of the brain slices for the classification of MRI brain images [1], [2]. In the aspect of image processing, the anatomically similarity of the brain slices can be treated as the similarity of brain slices in the viewing aspect along with the actual anatomical structure. This work aimed to prove that the consideration of the anatomical structure for the normal– abnormal classification will improve the result of the classification. In [3] the existing work shows that the feature vector, gray level co-occurrence matrix (GLCM) statistical features alongside support vector machine (SVM) and Back Propagating Neural Network (BPNN) produce better results than other methods. It uses multifractal segmentation along with intensity features as feature vector and classifier. Related works in current literatures for the normal/abnormal classification of MRI images does not consider the anatomical structure of the brain slices. Because of the dissimilarity in the anatomical structure, it may produce undesirable results.

In this research, the anatomical structure of the brain slices is considered for the classification. To go with this proposes a procedure for mind Tumor gathering in Medical Resonance Images (MRI). In this paper, CAD (Computer Aided

Diagnosis) framework is produced utilizing FDA features and machine learning based back propagation Neural Network and we are using Near Infrared Imaging Technology to detect the brain Tumor of the size below 3mm which could not be detected using CT [4] and MRI images and we transmit the thermal information through WSN. Infrared sensor is one of the successful electronic instrument which identifies certain qualities of its surroundings by either exuding or moreover distinguishing infrared radiation. Infrared sensors are in like manner prepared for evaluating the glow being delivered by a challenge and recognizing development. Highlight extraction is finished by utilizing dark level covariance network and further arrangement is finished by MLBPNN idea is presented here. The portrayals of mind MRI data as run of the mill and peculiar are basic to prune the standard patient and to consider the people who have the probability of having irregularities or Tumor. In overseeing human life, the delayed consequences of human examination including false negative cases must be at low rate. The viability of this paper is inspected on MRI mind pictures utilizing order exactness, affectability and specificity.

II. RELATED WORK

RaouiaAyachi *et al.* [5] primarily centers on division of MRI brain picture. In this paper principally consider the order issue where the goal of separate amongst unusual and ordinary pixels on the basic of various types of highlights, to be specific surface and powers. After this division procedure all the more precisely had done the arrangement procedure utilizing Support Vector Machine (SVM). In the test examine Gliomas dataset is utilized and this dataset has diverse picture powers, sizes, areas and tumor shapes..

El-Melegy *et al.* [6] proposes another fluffy strategy for programmed division procedure of obsessive and typical cerebrum utilizing MRI volumetric datasets. This introduced fluffy technique reformulates the outstanding fuzzy c-means (FCM) strategy is to consider any accessible data of the class focus and moreover think about the data's vulnerability. This data is utilized to regularize the bunches produced by fundamental FCM strategy hence, here enhancing its division execution under the sudden and boisterous conditions amid information securing. Moreover, quicken the fuzzy c-means calculation union process. This work utilizes both genuine and reproduced MRI images are extensive shows better outcomes in term of vigor, division precision.

Ay e *et al.* [7] proposes another tissue division calculation which is utilized to portions the brain MRI images into Gray Matter (GM), White Matter (WM), Cerebrospinal Fluid (CSF), Edema, and tumor. In this work utilize glial tumor's FLAIR MR, T2, and T1 images with 20 subjects. Before division process, in this work build up another calculation for stripping the skull and the Self-Organizing Map (SOM) is utilized for division process which is prepared by utilizing learning Vector Quantization (LVQ) with unsupervised learning calculation. Furthermore, in this work utilize Stationary Wavelet Transform (SWT) coefficients for build the info highlight vector as opposed to utilizing SOM extra system.

Xing *et al.* [8] proposes a learning-based system for programmed and hearty and core division with shape protection. In this work at first create a likelihood delineate utilizing Convolution Neural Network (CNN) for given core picture. After this procedure consolidating alocal loathsome deformable model and strong determination based scanty shape demonstrate for isolated the individual cores which is named as novel division calculation. In this work the three extensive scale pathology picture datasets are utilized for exploratory process and the trial comes about are demonstrates the predominant execution of this Convolution Neural Network (CNN) strategy where-as sensor.

Islam *et al.* [9] proposes a stochastic model for portraying the cerebrum tumor surface utilizing MR picture. In this work primarily focused on tumor division and highlight extraction on MRI picture. In light of the brain boggling appearance of the MRI picture, the surface of the cerebrum tumor picture is detailed by using a multiresolution-fractal display which is named as multifractional Brownian movement (mBm). After this procedure the division is finished by utilizing multifractal highlight based brain tumor division drew closer is created. This procedure is finished by utilizing multifractal highlights. Also, the Ada Boosting calculation is utilized for novel free tumor division process. Essential Ada Boosting calculation is altered by relegating weights to segment classifiers relies upon their arrangement capacity. Here 14 patients with more than 300 MRI picture are utilized for exploratory process and this procedure contrasted and poor quality glioma BRATS2012 dataset images, and the trial comes about shows normal and more steady outflanks of work.

Gravina *et al.* [10] proposes when in doubt, BSN development is advancing to multi-contraption synchronous estimation conditions; blend of the data from various, possibly heterogeneous, sensor sources is subsequently transforming into a urgent yet non-unimportant errand that clearly impacts application execution. The survey moreover covers data blend in the territories of feeling affirmation and general-prosperity and presents imperative headings and challenges of future research on multi-sensor mix in the BSN space.

Farahani *et al.* [11] recommends there is a change from the inside driven treatment to quiet driven human administrations where each specialist, for instance, recuperating office, patient, and organizations are reliably connected with one another. This patient-driven IoT eHealth normal framework needs a multi-layer building: (1) device, (2) haze getting ready and (3) cloud to empower treatment of complex data with respect to its social event, speed, and torpidity. We by then finally address the challenges of IoT eHealth [12], for instance, data organization, flexibility, bearings, interoperability, security, device– network– human interfaces and insurance. From the survey it concluded that the effectiveness accuracy, sensitivity and specificity on MRI brain images needs to concentrate which can be overcome using modular machine learning based neural networks.

Further Wireless Infrared Imaging Sensor is considered essential along with biosensor to transmit the tumor thermal information for remote access.

III. MATERIALS AND METHODS

A. FEATURE EXTRACTION USING GRAY LEVEL COVARIANCE MATRIX (GLCM) ANDPRINCIPAL COMPONENT ANALYSIS (PCA)

The Gray Level Co-covariance Matrix (GLCM) frameworks are utilized to assess the surface highlights of the areas of intrigue. Twenty textural features like autocorrelation, imperativeness, separate; relationship, entropy and homogeneity were segregated from the specific MRI cerebrum pictures and isolated utilizing the surface normal of four headings and separation. Then the extracted features are listed as follows. Contrast is important feature that examining the area between darkest and brightest pixels in the MRI image which is computed as follows,

$$contrast = \sum_{i,j=0}^{n-1} P_{ij}\,(\text{i-j})^2 \tag{1}$$

$$Dissimilarity = \sum_{i,j=0}^{n-1} |i-j|\,P(i,j) \tag{2}$$

$$Entropy = \sum_{i,j=0}^{n-1} -\ln\left(P_{ij}\right)P_{ij} \tag{3}$$

The homogeneity is used to measure compactness of pixels in image that is estimated using eqn 4.

$$Homogeneity = \sum_{i,j=0}^{n-1} \frac{P(i,j)}{1+(\text{i-j})^2} \tag{4}$$

Relationship between two variables are computed for determining the correlation that is done as,

$$correlation = \sum_{i,j=0}^{n-1} P_{ij}\frac{(i-\mu)(j-\mu)}{\sigma^2} \tag{5}$$

$$Energy = \sum_{i,j=0}^{n-1} \left(P_{ij}\right)^2 \tag{6}$$

The principal component analysis (PCA) is one of the effective procedures which utilized for picture acknowledgment and pressure. The reason for PCA is to diminish the substantial dimensionality of the information recovered from the sensor [13], [14] In Probabilistic neural network (PNN) classifier helps for Tumor classification which produced good results than the adaboost classifier. However there are problems in Back propagation (BP) Learning. Back spread has a few issues related with it which incorporate system loss of motion, nearby minima and moderate intermingling. Perhaps the best known is designated "Nearby Minima." This happens in light of the fact that the calculation dependably changes the weights so as to make the mistake fall. Be that as it may, the blunder may quickly need to ascend as a major aspect of a more broad fall, If this is the situation, the calculation will "stall out" (on the grounds that it can't go tough) and the mistake won't diminish further, Network loss of motion happens when the weights are changed in accordance with expansive qualities amid preparing, extensive weights can drive the vast majority of the units to work at extraordinary qualities, in an area where the subsidiary of the initiation work is little and multilayer neural system requires many rehashed introductions of the information designs, for which the weights should be balanced before the system can settle down into an ideal arrangement. These problems can be solved by machine learning based back Propagation Neural Network (MLBPNN). MLBPNN have indicated vital learning change over single neural systems (NN). Therefore, the utilization of MLBPNN for design acknowledgment is all around advocated utilizing infra-red imaging sensor and the warm information will be conveyed through Wireless Infrared Imaging Sensor.

B. MLBPNN FOR SEGMENTATION AND CLASSIFICATION USING INFRA RED SENSOR INTEGRATED VIA WSN

Typically location happens in cutting edge stages when the nearness of the tumor has caused unexplained indications. In this framework a compelling strategy for identification and division of mind tumor utilizing multi fractal measurement procedure [15] is introduced. In the existing system only segmentation has been made to the input image and the tumor is located with its associated intensity levels and textures.[16] The segmentation results also shows that the Ground truth, Dice Overloap, Jaccard index, False Positive and Negative index Fractions. Extracting White matter (WM), cerebrospinal fluid (CSF), gray matter (GM) is one of major issue. In t the complex image of the brain is extracted using Multi Fractal detection. The Figure .1.depicts the Overall flowchart of the system.

According to figure 2 Feature extraction is the stage in which the intensity features are derived [17] from given input image. To extract the features, fractal dimension algorithm is applied. Initially the image is split into number of blocks which are called sub images and also the divided blocks should not be overlapped. Then for each block extract the intensity texture features stored in the database. By using the intensity value, image histogram is extent as follows,

$$normalized\ histogram = \frac{number\ of\ pixels\ with\ intensity}{total\ number\ of\ pixels} \tag{7}$$

Then by taking this feature values as the ground truth the classification can be done.

Figure 3 depicts the segmented result of the Brain tumor image. This is ordinarily used to distinguish objects or other significant data in advanced pictures. The consequence of picture division is an approach of pieces that everything considered cover the whole picture, or a game-plan of shapes isolated from the photo.

$$\boldsymbol{Function}[\boldsymbol{output\_image\ x\ y}] = \boldsymbol{contour\_draw\_function}(\boldsymbol{input\_image}) \tag{8}$$

As explained in the eq.8 every pixel in a locale is comparative to some trademarks, like shading, surface. Nearby areas are fundamentally unique as for the same characteristic(s).

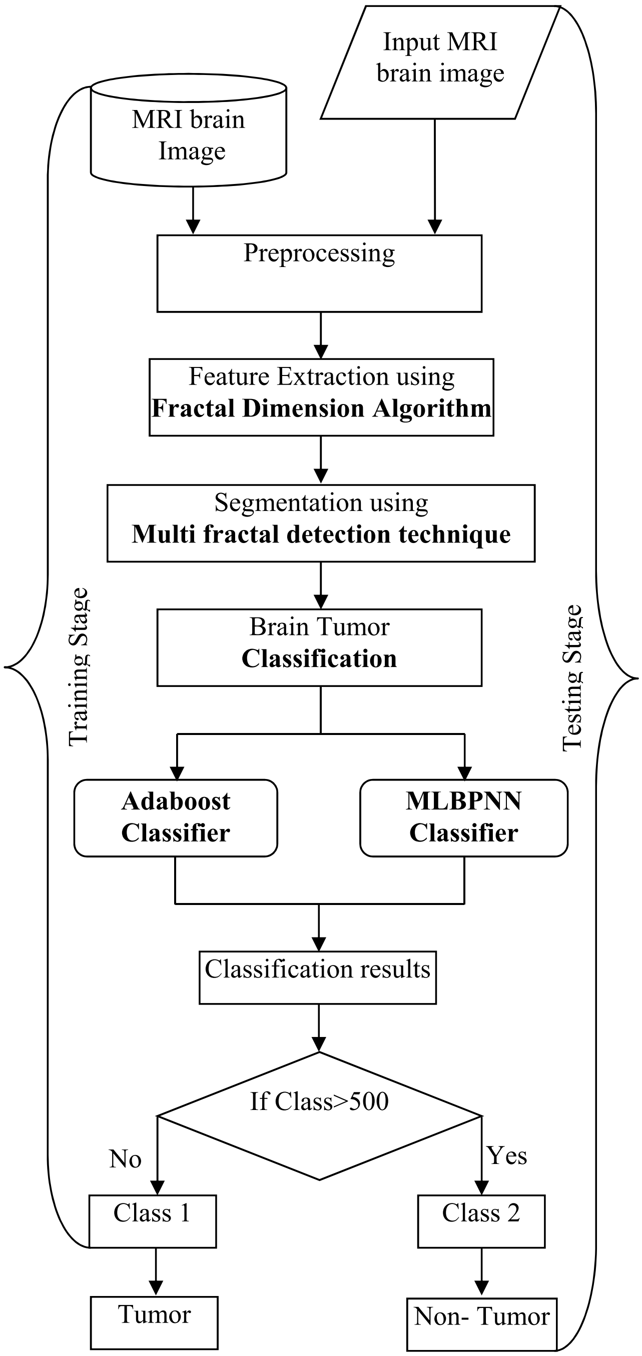

FIGURE 1. Overall structure of brain tumor detection and segmentation system.

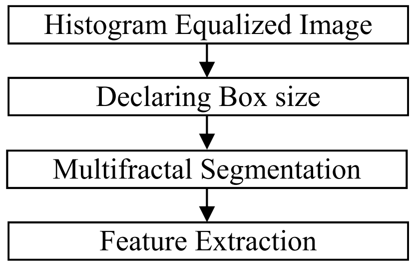

FIGURE 2. Process of feature extraction using FDA.

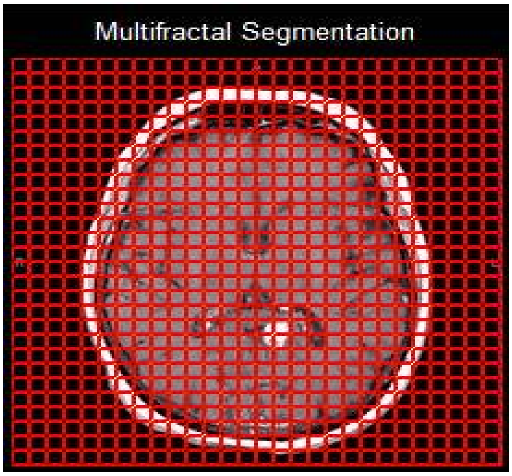

FIGURE 3. Segmented image using MFD.

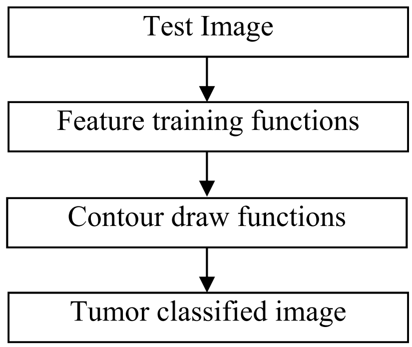

FIGURE 4. Steps of classification of tumor images.

1) CLASSIFICATION

Figure 4 Shows the classification steps where the extracted feature values decides whether the tissue is tumor one or not [18]. This can be done by comparing the feature values which extracted already from the ground truth and the feature extracted from the test images. Ada boost algorithm is used in classifying the tumor tissue from the input image. This is done in the iterative manner till the iteration equal to the no of divided blocks.

a: ADABOOST CLASSIFIER

AdaBoost, short for Adaptive Boosting, is a machine learning figuring characterized by Yoav Freund and Robert Schapire who attained the prestigious "Gödel Prize" in 2003 for their effort [19]. It is a meta-count, and can be used as a piece of combination with various other learning estimations to upgrade their execution. AdaBoost is flexible as in resulting classifiers built are altered for those illustrations misclassified by past classifiers. AdaBoost is fragile to rowdy data and inconsistencies. Where in PNN classifier is utilized for Tumor characterization which delivered great outcomes than the adaboost classifier. In addition to this, the Adaboost classifier enhance the tumor classification process as follows,

$$B_T(x) = \sum_{t=1}^{T} w_t(x) \tag{9}$$

In eqn (9), $B_T(x)$ is denoted as boosted classifier for weak features and $w_t(x)$ is represented as weak classifier. Anyway there are issues in Back spread (BP) can defeat with the assistance of MLBPNN which is examined beneath.

b: MLBPNN CLASSIFIER

The machine learning Back spread calculation neural systems searches for the most extreme of the mistake work in weight space utilizing the technique for slope drop. The blend of weight which limits the mistake work is thought to be an answer of the learning issue introduction. The back engendering calculation is utilized to locate the nearby least of the mistake work. The system is introduced with arbitrarily picked weights. The inclination of the blunder work is registered and used to adjust the underlying weights. The assignment is to figure this angle recursively. There is a need to make a framework and to set the synaptic weights to some subjective characteristics. Amid this procedure the yield of the system layer is gotten as takes after. Each neuron network is computed as,

$$O_{pj}\left(net_j\right) = \frac{1}{1+e^{-\lambda net_j}} \tag{10}$$

In eq n (10)), the net_j value is estimated as,

$$net_j = b * w_b + \sum_k O_{pk} w_{kj} \tag{11}$$

Un eqn (11), b is represented as bias, wb is weight of the bias value, wkj is the weight between the link k and j in network.

Before performing the output of particular input network utilizes the response function as sigmoid function to train the network to get the effective results which is estimated as follows.

$$f(x) = \frac{1}{1+e^{-\lambda x}} \tag{12}$$

2) FEED FORWARD THE TRAINING PATTERNS

The network handling testing and training dataset.

Neural networks depicted in Fig (5) are determining strategies that depend on simple mathematical models of the brain. They permit complex nonlinear connections between the reaction variable and its indicators.

The weighted edges [21] are utilized as a part of the very same path in the two stages: they regulate the data transmitted toward every path by duplicating it by the edge's weight.

Figure 6 shows the Overall processing steps of Back Propagating Neural Network.

3) TRAINING THE IMAGES

Once a framework has been composed the basic weights are picked erratically. Then, the arrangement, or learning, begins. After that the output estimation process, the network propagate the error value which is estimated as,

$$\delta_{pj} = \left(T_{pj} - O_{pj}\right) O_{pj}(1 - O_{pj}) \tag{13}$$

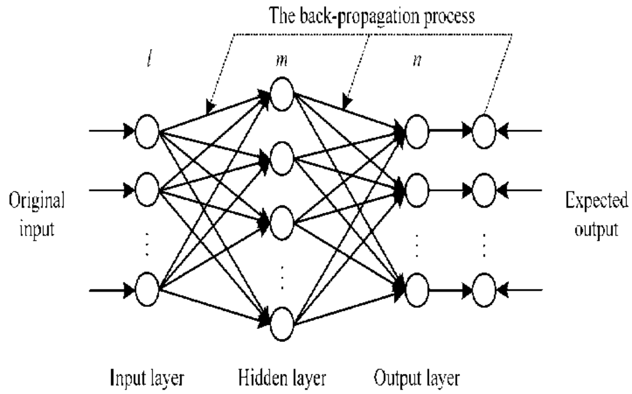

FIGURE 5. Structure of back propagation neural networks.

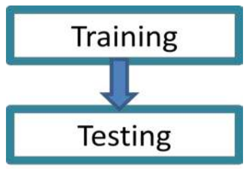

FIGURE 6. Processing steps of BPNN.

In eqn (13), T_{pj} is output neuron target value in particular pattern p.

O_{pj} is actual output value of j output neuron in pattern p.

In addition ot this output neuron error value, hidden layer error value also estimated as,

$$\delta_{pj} = O_{pj}(1 - O_{pj}) \sum_k \delta_{pk} w_{kj} \tag{14}$$

IN eqn (14), δ_{pk} denoted as error value of post synaptic neuron k and wkj is weight value of linj k and j.

According to the propagated error value, the weight has to be updated as follows,

$$\Delta w_{ji}(t) = \eta \delta_{pj} O_{pi} \tag{15}$$

From the computed weight adjustment value, it has been utilized to update and generate new weight value as follows.

$$w_{ji}(t+1) = w_{ji}(t) + \Delta w_{ji}(t) \tag{16}$$

As shown in the Figure.7. There are two different ways to manage getting ready - directed and unsupervised. Coordinated planning incorporates an instrument of outfitting the framework with the pined for yield either by physically "assessing" the framework's execution or by giving the pined for yields the data sources. Unsupervised planning is the place the framework needs to comprehend the commitments without outside help. The enormous larger piece of frameworks utilize coordinated getting ready. Unsupervised planning is used to play out some basic depiction on inputs. Division system for Magnetic Resonance Imaging (MRI) [22] of the mind is one of the strategy utilized by radiographer to identify any irregularity happened particularly for cerebrum.

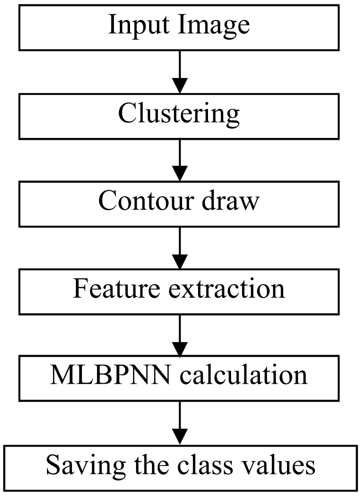

FIGURE 7. **Training image analysis steps.**

Clustering algorithm is one of the processes in segmentation followed by feature extraction and MLBPNN calculation for saving class values.

4) CLUSTERING

Clustering or grouping [23] is basically an arrangement of such bunches, typically containing all items in the informational index. Also, it might indicate the connections of the groups to each other. For instance, a pecking order of groups implanted in each other. Grouping can be generally recognized as:

- hard grouping – each question has a place with a bunch or not
- soft grouping – each protest has a place with each bunch to a specific degree

Grouping calculation can be ordered as in view of their bunch show.

5) CONTOUR DRAW

Contours are frequently gotten from edges, however they are gone for being object Contours. In this way, they should be closed curves. You can consider them limits Thus, they need to be closed curves. You can think of them as boundaries [24]. Along these lines, the measure of calculation is incredibly decreased when we run highlight separating calculations on the shape rather than all in all example.

$$\text{Function}[output\_image\ x\ y] = contour\_draw\_function(input\_image)$$

Figure 8(a) demonstrates the contour Initialization image and Figure 8(b) demonstrates the manual segmented image. Since the shape imparts a considerable measure of highlights to the first example, the element extraction process turns out to be substantially more proficient when performed on the form rather on the first example.

$$\text{Function}[output\_image\ x\ y] = contour\_draw\_function(input\_image)$$

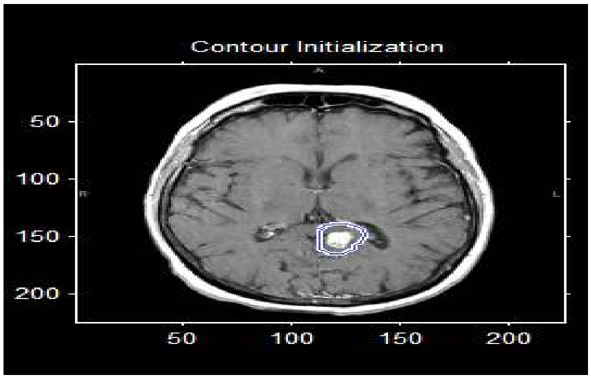

(a)

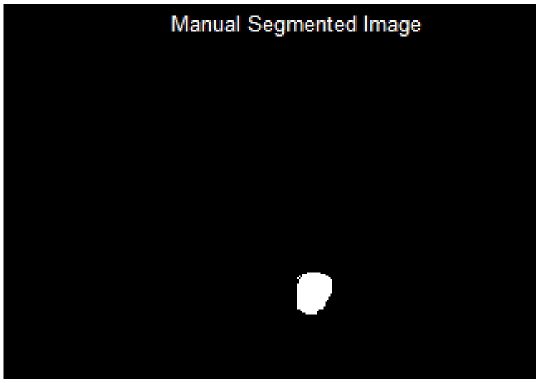

(b)

FIGURE 8. **(a) Contour initialization. (b) Manual segmented image.**

6) FEATURE EXTRACTION

Feature extraction [25] includes streamlining the proportion of benefits recovered to portray an immense plan of data exactly. When performing examination of complex information one of the vital issues starts from the no of components included. Examinations with a significant no of variable all things considered requires a great deal of memory and computation control or a gathering estimation which over fits the arrangement test and entireties up ineffectually to new illustrations. It is a general term for systems for building blend of the components to get around these issues although up 'til now portraying the data with satisfactory precision.

7) MLBPNN CALCULATION

The back propagation neural network is utilized to implement the brain tumour classification process

Once the values are calculated it is detected through Infrared which is utilized to predict different attributes in environment that has to be transmitted via infrared radiation. Infrared sensors are also fit for evaluating the warmth being transmitted by a dissent and recognizing development and master clinician to screen the wellbeing condition however remote [26] sensor arrange through distributed storage for remote access.

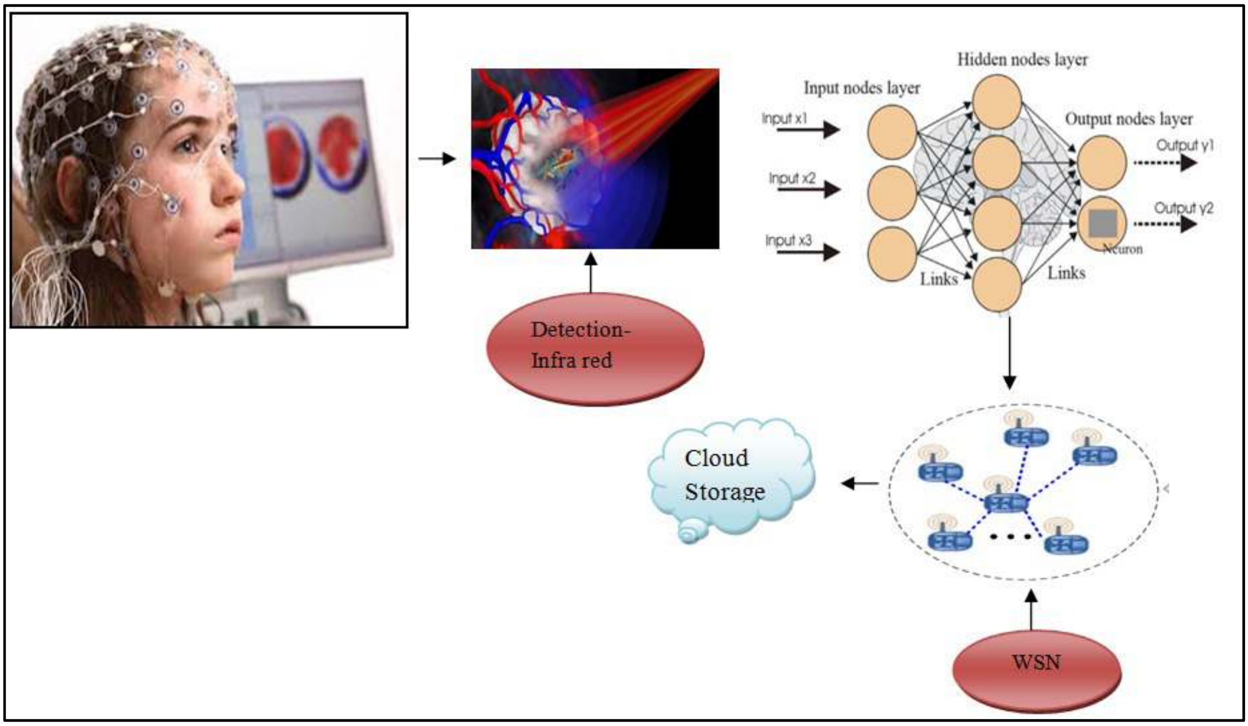

FIGURE 9. Structure of the modular machine learning based Back propagation neural network architecture.

As shown in the Figure 9. The machine learning based Back propagation neural network scheme contains of a level of input components which consists of infra-red sensor for sensing the brain images and an additional decision module. All sub-systems are MLPs Every information variable is associated with just a single of the information modules These associations are picked indiscriminately the yields of all information modules are associated with the choice system. In distributed computing condition, it is presently conceivable to screen and accumulate physical data through heaps of sensor nodes to meet the prerequisites of cloud administrations. By and large, those sensor hubs gather information and send information to sink hub where end-clients can question all the data and accomplish cloud applications through WSN for remote access.

8) TESTING

The introduced neural network successfully works on testing dataset without involvement of training set.

The testing set can be viewed as the delegate instances of the general wonder. On the off chance that the system works good on testing dataset it can be required to works well on general case. The Figure.10 shows the Flowchart for Testing in MLBPNN.

a) Holes Filling - The objective is to eliminate reflections by hole filling. As shown in the Eq.17

$$\boldsymbol{locator} = \boldsymbol{imfill}(\boldsymbol{locator}, \text{'}\boldsymbol{holes}\text{'}); \tag{17}$$

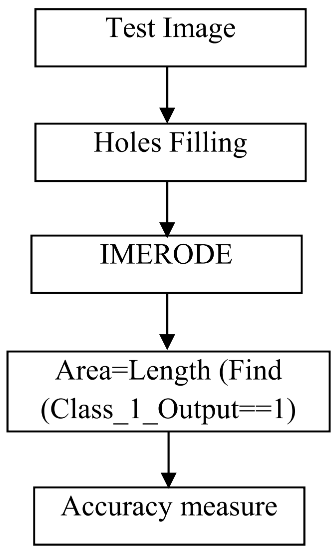

FIGURE 10. Testing image analysis steps.

b) Erosion –is process of measuring the shape of fitness of image which helps to predict how the images are changed from their original shape. As shown in the Eq.18

$$\boldsymbol{eroded} = \boldsymbol{imerode}\,(\boldsymbol{locator}, \boldsymbol{se})\,; \tag{18}$$

c) Declaring the Class Size Every tumor has different size and it is very difficult to extract the features for higher areas. So we are defining the class values in a

Algorithm 1

Initialize the MRI images, features

Step 1: Read the input MRI image

Step 2: Analyze the age gap of image and divide into training TR image and Testing TE image.

Step 3: Extract the features (area, perimenter, circularity, equiv diameter, eccentricity, major axis, minor axis, min intensity and max intensity)

Step 4: Fed the input the MLBPNN classifier.

Step 5: Compute output of each neuron as follows,

$$O_{pj}\left(net_j\right) = \frac{1}{1+e^{-\lambda net_j}}$$
$$net_j = b * w_b + \sum_k O_{pk} w_{kj}$$

Step 7: Check if the output is having error or not by comparing actual and estimated output in both output and hidden neuron as follows,

$$\delta_{pj} = \left(T_{pj} - O_{pj}\right) O_{pj}(1 - O_{pj}) \text{ (output neuron error)}$$
$$\delta_{pj} = O_{pj}(1 - O_{pj}) \sum_k \delta_{pk} w_{kj} \text{ (hidden neuron output)}$$

Step 8: If the network having error it has to be propagate and minimize by weight update process.

$$\Delta w_{ji}(t) = \eta \delta_{pj} O_{pi}$$

Step 9: Update weight value as follows,

$$w_{ji}(t+1) = w_{ji}(t) + \Delta w_{ji}(t)$$

Step 10: Repeat this process until to get the output value of given input.

way that if

$$\begin{gathered} \textbf{\textit{if area}} < 500 \\ \textbf{\textit{disp}}(\textbf{\textit{Class}} - \mathbf{1}'); \\ \textbf{\textit{else}} \\ \textbf{\textit{disp}}(`\textbf{\textit{Class}} - \mathbf{2}'); \\ \textbf{\textit{end}} \end{gathered}$$

The testing dataset consist of several cases that used to how effectively tumour is recognized in both testing as well as general cases.

d) **Accuracy Calculation** Accuracy is the extent of genuine outcomes (both genuine positives and genuine negatives) in the populace. To make the setting unmistakable by the semantics, usually alluded to as the "Rand Accuracy." It is a parameter of the test as shown in the eq.19, as shown at the bottom of this page.

The output of all parameters measured and the output of MLBPNN has been discussed below.

IV. RESULTS AND DISCUSSION

Brain tumor is an anomalous development of cells inside the mind or in the focal spinal waterway. A MRI [27] Brain tumor picture is taken as info. As an underlying advance preprocessing, this is being done by utilizing Standard Median Filter so as to expel the Salt and Pepper Noise. Picture Enhancement is finished with the assistance of difference extending (Histogram Equalization) by consistently re-conveying the dim qualities. This is followed by Segmentation using Multi Fractal .Then Classification is done using two techniques Adaboost Classifier and machine learning based Back Propagating Neural Network. In Adaboost classifier the tumor is classified using Intensity Features where as in BPNN, classification is done based on the tumor area. Comparing to Adaboost, MLBPNN has an additional advantage of detecting whether the tumor is in early stage or in advanced stage. Finally performance of Adaboost Classifier and Back Propagating Neural Network has been compared.

A. EVALUATION CRITERIA

This section depicted that the sample brain tumour related images. During this analyse process, the machine learning based Back propagation neural network utilizes 30 sample images for making the tumour classification process. Then the sample MRI brain image is shown in figure 11.

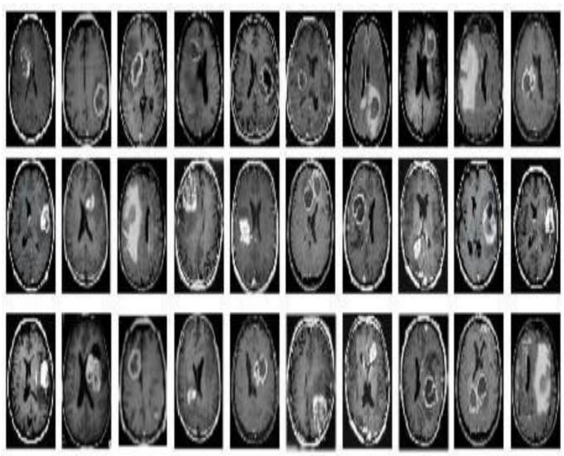

FIGURE 11. Samples of the MRI data base.

As shown in the Figure.11. The location of tumor is estimated as far as affectability, specificity and Accuracy which are broadly used to assess the execution of

$$\textit{accuracy} = \frac{\textit{number of true positives} + \textit{number of true negatives}}{\textit{number of true positives} + \textit{false positives} + \textit{false negatives} + \textit{true negatives}} \tag{19}$$

TABLE 1. Class I database for MLBPNN.

CLASS 1	Case 1	Case 2
Area	210	184
Perimeter	56	55
Circularity	0.509054	0.327694
Equiv Diameter	16.35177	15.30608
Eccentricity	0.84265	1.178316
Major axis	17	17
Minor axis	13	11
Min_ Intensity	78	98
Max _ Intensity	255	255

TABLE 2. Class II database for MLBPNN.

CLASS II	Case 1	Case 2	Case 3
Area	501	691	859
Perimeter	89	114	167
Circularity	0.52031	1.585713	1.332656
EquivDiameter	25.25654	29.66157	33.07133
Eccentricity	0.539743	0.765333	0.761845
Major axis	25	34	44
Minor axis	22	27	35
Min_ Intensity	100	37	126
Max _ Intensity Extracted Features	255	182	255

the Medical picture arrangement. Region and different parameters are likewise used to assess the execution of Classification.

Where TP is the quantity of Positive examples effectively arranged, FN is the quantity of Positive example in accurately named Negative, TN is number of Negative examples accurately [28] grouped and FP is the quantity of Negative examples inaccurately named Positive.

High affectability implies high capacity of recognizing tumor. High specificity implies high ability of dodging

TABLE 3. Confusion matrix for MLBPNN.

ACTUAL	PREDICTED	
	MLBPNN Algorithm 30 tested images 9 Normal Images and 21 Abnormal Images(Figure.1)	
	Abnormal (Positive)	Normal (Negative)
Abnormal (Positive)	TP(19)	FP(2)
Normal (Negative)	FN(1)	TN(8)

TABLE 4. Comparison of adaboost classifier and MLBPNN.

PARAMETERS	Adaboost Classifier	MLBPNN
Accuracy	67.15	93.33
Sensitivity	68.18	71.42
Specificity	53.04	88.88
Area	NA	210
Perimeter	NA	56
Circularity	NA	0.509054
Equiv Diameter	NA	16.35177
Eccentricity	NA	0.84265
Major axis	NA	17
Minor axis	NA	13
Min Intensity	NA	78
Max Intensity	NA	255

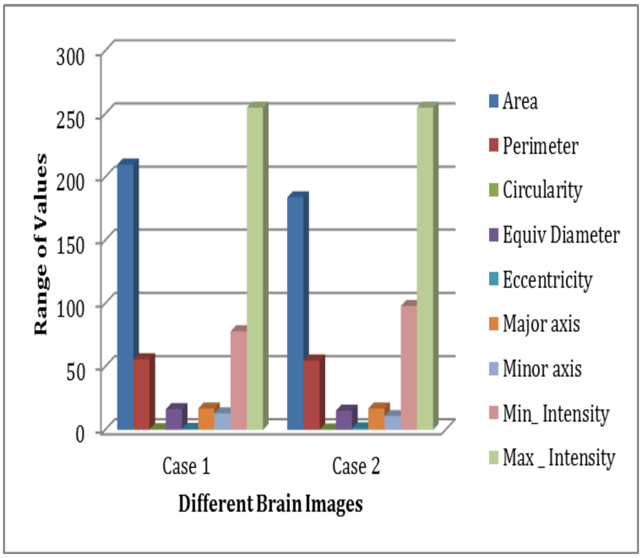

FIGURE 12. Comparison for the Class I extracted features for MLBPNN.

false recognition. Exactness is utilized to assess the general execution of the machine learning based back propagation neural network strategy. Since CAD is utilized to

TABLE 5. Comparison of various tumor classification methods.

Surgical Planning Laboratory (SPL) dataset	Traditional approach [24]		k-Nearest Neigbor [25]		(Extreme Learning Machine Approach approach)[26]		Machine Learning Based Back Propagation Neural Network	
	Sensitivity	Specificity	Sensitivity	Specificity	Sensitivity	Specificity	Sensitivity	Specificity
Case 1	100	100	100	100	99.9	100	100	100
Case 2	82.2	99.9	94.8	88.8	99.9	99.8	98.8	99.9
Case 3	93.6	94	89.8	96	94.56	99.8	95.61	99.8
Case 4	83.3	95	83.3	96	92.4	91	93.6	99.9
Case 5	89.3	89.9	83.8	96	90.6	98.6	95.2	99.8
Case 6	90.5	95.9	96	86.8	93.5	98.6	96.9	99.9
Case 7	94.6	95.9	94.8	87.8	94.2	97.8	96.1	99.8
Case 8	83.6	95.9	93.1	88.8	89.6	97.4	94.1	99.9
Case 9	91.8	94.9	99.3	89.8	96.9	97.5	99.92	99.8
Case 10	98.8	92	95.6	88.8	96.9	97.6	99.4	99.9
Average	88.68	93.9	91.02	87.8	91.506	96.81	95.103	99.8

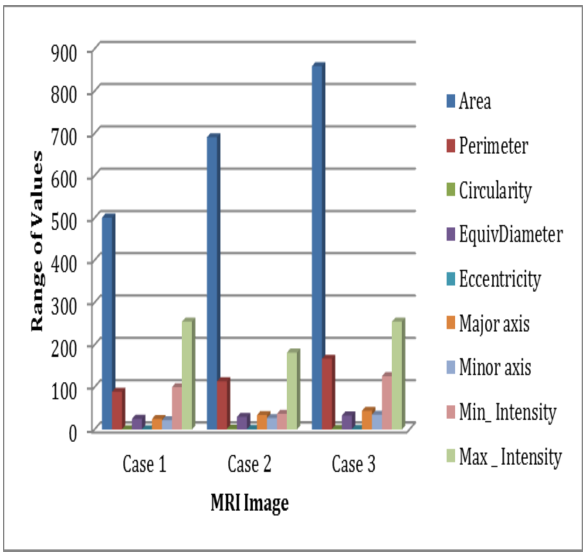

FIGURE 13. Comparison of Class II extracted features for MLBPNN.

recognize tumor and send them to clinicians for particular examinations, affectability is more imperative than specificity and exactness.

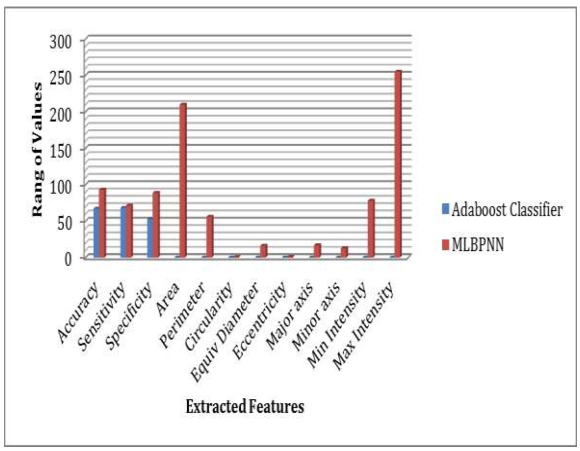

FIGURE 14. Optimized parameter comparison for adaboost classifier and MLBPNN.

B. SAVING THE CLASS VALUE FOR MLBPNN

The next part of the flowchart is saving the class values considering the tumor size for separating the class values. If the tumor area size is less than 500 then it is said to be

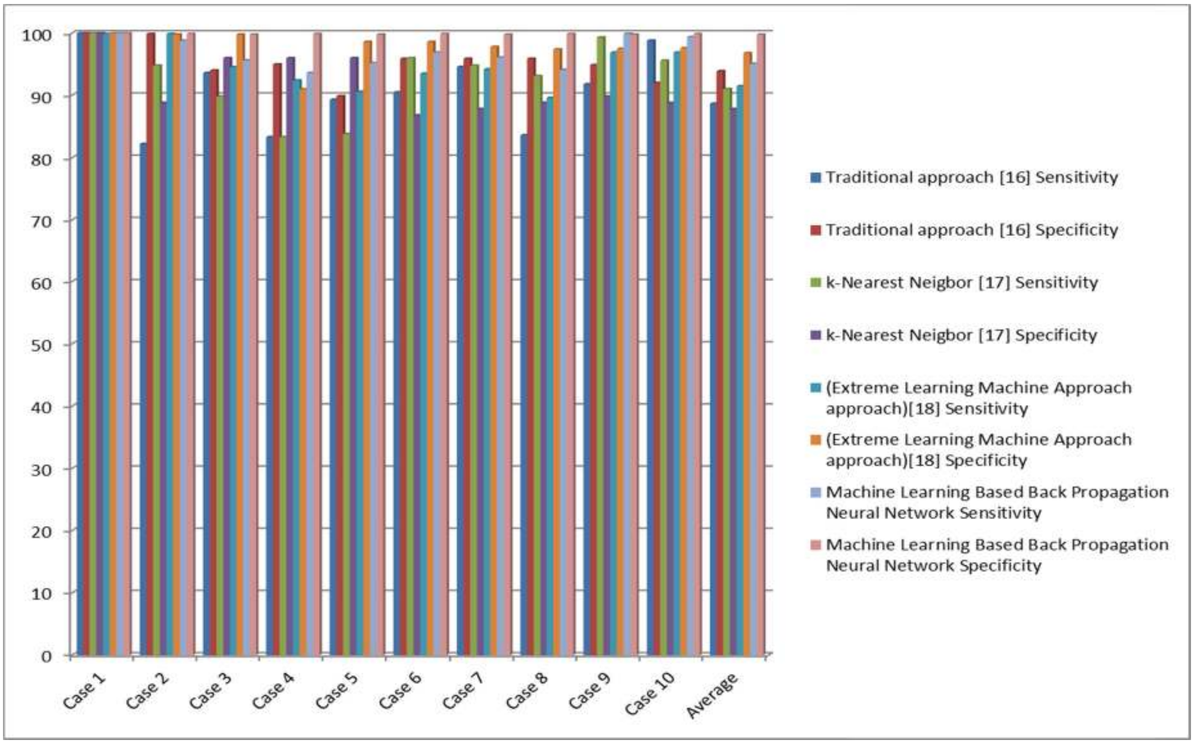

FIGURE 15. **Representation of tumor prediction methods with modular machine learning based neural networks.**

class 1. Then a Database value for *Class I* is created and stored for the future use. For classifying the brain tumor [29] training is the important part. Wherein Table.1 shows the features of the *Class I* images.

The above table 1 demonstrate that multi-layer back propagation neural network process different MRI brain image features such as area, perimeter, circularity, intensity values with effective manner. The effective utilization of brain features helps to predict brain tumors successfully and the analyse of the class I database image result is shown in figure 12.

Figure 12 shows the comparison for the Class I extracted Features [30] in case if the tumor area size is greater than 500, then database value is created and stored for Class II functions as illustrated in the Table. 2.

Table 2 contains the different class II image related feature information, the database consists of collection of images which has size in above 500 that too identified and analysed effectively while classifying brain tumors and related graphical representation is shown in figure 13.

The performance of the MLBPNN features is compared as shown in the Figure.13 The randomly selected 21 tumor images and 9 non tumor imageries as of the database for training and other for testing. The predicted confusion matrix related values such true positive, false positive, true negative and false negative is shown in below in Table.3.

The Classification result using MLBPNN are shown in Table.4 for 30 images. Apparently, the feature extraction shows much better discrimination ability for detecting tumours' from the other features. The Table.4 shows the Comparison of Adaboost and MLBPNN classifier.

Table 4 depicted that comparison of Adaboost and multi-layer back propagation neural network feature extraction comparison process. From the comparison, it clearly shows that multi-layer back propagation neural network effectively process the extracted features such as specificity, area, perimeter, intensity, circularity also attains the high accuracy value while classifying brain tumors. According to the above obtained results the pictorial demonstration of the value is depicted in figure 14.

The Figure 14 shows the Performance optimized parameter comparison Graph for Adaboost Classifier and MLBPNN.Brain tumor detection technique used to developing automatic tumor detection and treatment examination process. The tumor area is considered to predict abnormality of brain tumor from MRI brain image. Then the performance of MRI brain tumor detection efficiency is measured using Sensitivity, Specificit and Accuracy [31] parameters. The performance of Adaboost Classifier and Back Propagating Neural Network has been compared.

The machine learning based Back propagation neural network model attains effective results for entre 10 SPL dataset cases and shown in table 5.

Both expert and neural network based tumor segmented result is shown figure 15. Here the performance of detecting

Brain tumor MRI images is measured in terms of Sensitivity and Specificity for various cases.

V. CONCLUSION

The machine learning based Back propagation neural network system is of highly practical values in realizing information and segmenting the tumour image. In MLBPNN, the two main processes are training and testing. The tumor images are classified further as class I database if area < 500 and as Class II Database if area > 500. In testing, the image to be tested is gone through holes filling. This enables the region around tumor to be filled and only the tumor part to be highlighted. Imerode function helps to locate the tumor exactly. Area of tumor is calculated and thus classified as class I or Class II and its accuracy is also estimated. The comparison between Adaboost Classifier and the machine learning based Back Propagating Neural Network on the following parameters has been made. From the values obtained it can be concluded that machine learning Back Propagating Neural Network is more efficient than the Adaboost Classifier. Though the 2D image segmentation methods can give accurate results, this will lose some of the geometric Information. So there is a need to study about 3D Brain medical imaging using machine learning methodologies in Future using this infra red sensor imaging techniques in WSN environment.

REFERENCES

[1] A. Kassner and R. E. Thornhill, "Texture analysis: A review of neurologic MR imaging applications," *Amer. J. NeuroRadiol.*, vol. 31, pp. 809–816, May 2010.

[2] G. W. Jiji, L. Ganesan, and S. S. Ganesh, "Unsupervised texture classification," *J. Theor. Appl. Inf. Technol.*, vol. 5, no. 4, pp. 373–381, Apr. 2009.

[3] K. V. Ramana and B. R. Korrapati, "A neural network based classification and diagnosis of brain hemorrhages," *Int. J. Artif. Intell. Expert Syst.*, vol. 1, no. 2, 2009.

[4] P. P. R. Filho *et al.*, "Automated recognition of lung diseases in CT images based on the optimum-path forest classifier," *Neural Comput. Appl.*, pp. 1–14, Jun. 2017.

[5] R. Ayachi and N. B. Amor, "Brain tumor segmentation using support vector machines," *Proc. 10th Eur. Conf. (ECSQARU)*, vol. 5590. Berlin, Germany: Springer, 2009, pp. 736–747.

[6] M. T. El-Melegy and H. M. Mokhtar, "Tumor segmentation in brain MRI using a fuzzy approach with class center priors," *EURASIP J. Image Video Process.*, vol. 21, no. 1, pp. 2–14, 2014.

[7] A. Demirhan, M. Törü, and I. Güler, "Segmentation of tumor and edema along with healthy tissues of brain using wavelets and neural networks," *IEEE J. Biomed. Health Inform.*, vol. 19, no. 4, pp. 1451–1458, Jul. 2015.

[8] F. Xing, Y. Xie, and L. Yang, "An automatic learning-based framework for robust nucleus segmentation," *IEEE Trans. Med. Imag.*, vol. 35, no. 2, pp. 550–566, Feb. 2016.

[9] A. Islam, S. M. S. Reza, and K. M. Iftekharuddin, "Multifractal texture estimation for detection and segmentation of brain tumors," *IEEE Trans. Biomed. Eng.*, vol. 60, no. 11, pp. 3204–3215, Nov. 2013.

[10] R. Gravina, P. Alinia, H. Ghasemzadeh, and G. Fortino, "Multi-sensor fusion in body sensor networks: State-of-the-art and research challenges," *Inf. Fusion*, vol. 35, pp. 68–80, May 2017.

[11] B. Farahani, F. Firouzi, V. Chang, M. Badaroglu, N. Constant, and K. Mankodiya, "Towards fog-driven IoT eHealth: Promises and challenges of IoT in medicine and healthcare," *Future Gener. Comput. Syst.*, vol. 78, pp. 659–676, Jan. 2018.

[12] P. M. Shakeel, S. Baskar, V. R. S. Dhulipala, S. Mishra, and M. M. Jaber, "Maintaining security and privacy in health care system using learning based deep-Q-networks," *J. Med. Syst.*, vol. 42, p. 186, Oct. 2018.

[13] G. S. N. Murthy and T. Veerraju, "A novel approach based on decreased dimension and reduced gray level range matrix features for stone texture classification," *Int. J. Elect. Comput. Eng.*, vol. 7, no. 5, pp. 2502–2513, 2017.

[14] F. J. Martinez-Murcia *et al.*, "On the brain structure heterogeneity of autism: Parsing out acquisition site effects with significance-weighted principal component analysis," *Hum. Brain Mapping*, vol. 38, no. 3, pp. 1208–1223, 2017.

[15] B. H. Menze *et al.*, "The multimodal brain Tumor image segmentation benchmark (BRATS)," *IEEE Trans. Med. Imag.*, vol. 34, no. 10, pp. 1993–2024, Oct. 2015.

[16] M. Ji *et al.*, "Detection of human brain Tumor infiltration with quantitative stimulated Raman scattering microscopy," *Sci. Transl. Med.*, vol. 7, no. 309, p. 309ra163, 2015.

[17] D. Wang, D. Miao, and C. Xie, "Best basis-based wavelet packet entropy feature extraction and hierarchical EEG classification for epileptic detection," *Expert Syst. Appl.*, vol. 38, no. 11, pp. 14314–14320, 2011.

[18] F. N. Karameh and M. A. Dahleh, "Automated classification of EEG signals in brain tumor diagnostics," in *Proc. IEEE Amer. Control Conf.*, Chiago, IL, USA, Jun. 2000, pp. 4169–4173.

[19] S. Yang, L. F. Chen, T. Yan, Y. H. Zhao, and Y. J. Fan, "An ensemble classification algorithm for convolutional neural network based on AdaBoost," in *Proc. IEEE/ACIS 16th Int. Conf. Comput. Inf. Sci. (ICIS)*, May 2017, pp. 401–406.

[20] I. S. Samant, G. K. Kanungo, and S. K. Mishra, "Desired EEG signals for detection brain tumor using LMS algorithm and feedforward network," *Int. J. Eng. Trends Technol.*, vol. 3, no. 6, pp. 718–723, 2012.

[21] Y. Fu *et al.*, "Network topologies and dynamics leading to endotoxin tolerance and priming in innate immune cells," *PLoS Comput. Biol.*, vol. 8, no. 5, p. e1002526, 2012.

[22] G. P. Rathi and S. D. Palani, "Brain tumor MRI image classification with feature selection and extraction using linear discriminant analysis," *Int. J. Inf. Sci. Techn.*, vol. 2, no. 4, p. 146, 2012.

[23] U. Orhan, M. Hekim, and M. Ozer, "EEG signals classification using the K-means clustering and a multilayer perceptron neural network model," *Expert Syst. Appl.*, vol. 38, no. 10, pp. 13475–13481, 2011.

[24] P. P. R. Filho, P. C. Cortez, A. C. da Silva Barros, V. H. C. Albuquerque, and J. M. R. S. Tavares, "Novel and powerful 3D adaptive crisp active contour method applied in the segmentation of CT lung images," *Med. Image Anal.*, vol. 35, pp. 503–516, Jan. 2017.

[25] Y. Song and P. Liò, "A new approach for epileptic seizure detection: Sample entropy based feature extraction and extreme learning machine," *J. Biomed. Sci. Eng.*, vol. 3, no. 6, pp. 556–567, 2010.

[26] M. B. Rodrigues *et al.*, "Health of things algorithms for malignancy level classification of lung nodules," *IEEE Access*, vol. 6, pp. 18592–18601, 2018.

[27] Y. Cao, D. Li, Z. Shen, and D. Normolle, "Sensitivity of quantitative metrics derived from DCE MRI and a pharmacokinetic model to image quality and acquisition parameters," *Acad. Radiol.*, vol. 17, no. 4, pp. 468–478, 2010. [Online]. Available: https://www.ncbi.nlm.nih.gov/pmc/articles/PMC3932530/

[28] R. de Boer *et al.*, "Accuracy and reproducibility study of automatic MRI brain tissue segmentation methods," *NeuroImage*, vol. 51, no. 3, pp. 1047–1056, 2010.

[29] D. S. Nachimuthu and A. Baladhandapani, "Multidimensional texture characterization: On analysis for brain tumor tissues using MRS and MRI," *J. Digit. Imag.*, vol. 27, no. 4, pp. 496–506, 2014.

[30] R. Barzegar, A. A. Moghaddam, J. Adamowski, and B. Ozga-Zielinski, "Multi-step water quality forecasting using a boosting ensemble multi-wavelet extreme learning machine model," *Stochastic Environ. Res. Risk Assessment*, vol. 32, no. 3, pp. 799–813, 2018.

[31] S. Lu, Z. Lu, J. Yang, M. Yang, and S. Wang, "A pathological brain detection system based on kernel based ELM," *Multimedia Tools Appl.*, vol. 77, no. 3, pp. 3715–3728, 2018.

Authors' photographs and biographies not available at the time of publication.